^{13}C NMR Analysis of the Cysteine-Sulfenic Acid Redox Center of Enterococcal NADH Peroxidase†

Edward J. Crane, III,‡,§ Jacques Vervoort,‖ and Al Claiborne*,‡

Department of Biochemistry, Wake Forest University Medical Center, Winston-Salem, North Carolina 27157, and Department of Biochemistry, Agricultural University, Wageningen, The Netherlands

Received April 7, 1997; Revised Manuscript Received May 16, 1997⊗

ABSTRACT: In order to characterize the native Cys42-sulfenic acid redox center of the flavoprotein NADH peroxidase by NMR, an expression protocol has been developed which yields the [3-^{13}C]Cys42-labeled protein in 100 mg quantities. Difference spectra of the labeled minus unlabeled oxidized enzyme (E) give a peak at 41.3 ppm (relative to dioxane) which represents the Cys42-sulfenic acid. Reduction of labeled E with 1 equiv of NADH gives the air-stable two-electron reduced (EH_2) species, and oxidized minus reduced difference spectra give maxima and minima at 41.3 and 30.8 ppm, respectively, corresponding to the Cys42-sulfenic acid and -thiolate species. Peroxide inactivation of E, which has previously been attributed to oxidation of the Cys42-sulfenic acid to the Cys42-sulfinic and/or sulfonic acid states, gives rise to a new maximum in the difference spectrum of $E_{inactive}$ minus E at 57.0 ppm. A similar expression protocol was used to obtain the [*ring*-2-^{13}C]His-labeled peroxidase HHAA mutant (His_{10}-$His_{23}Ala_{87}Ala_{258}$); the spectral change over the pH range 5.8−7.8 is attributed to deprotonation of the surface-exposed His23. Furthermore, replacement of Arg303, which is hydrogen bonded to His10, has no effect on the ^{13}C spectrum. These results provide direct evidence in support of the peroxidase Cys42-sulfenic acid/thiol redox cycle and add significantly to our structure-based understanding of protein−sulfenic acid stabilization and function.

The flavoprotein NADH peroxidase from *Enterococcus faecalis* 10C1 contains, in addition to FAD, a cysteinyl redox center which undergoes reversible two-electron reduction (to Cys-SH) and oxidation by H_2O_2 during the catalytic cycle (*1*). The oxidized enzyme is reduced by NADH in an initial priming step; in the steady state the enzyme cycles between EH_2·NADH* and E·NADH forms:

$$E(FAD, Cys42\text{-}SOH) + NADH + H^+ \rightarrow EH_2(FAD, Cys42\text{-}SH) + NAD^+ + H_2O$$

$$EH_2 + NADH \xrightarrow{k_1} EH_2\cdot NADH^*$$

$$EH_2\cdot NADH^* + H_2O_2 \xrightarrow{k_3} E\cdot NADH + H_2O$$

$$E\cdot NADH + H^+ \xrightarrow{k_4'} EH_2\cdot NAD^+ + H_2O$$

$$EH_2\cdot NAD^+ \underset{k_1'}{\overset{k_2'}{\rightleftharpoons}} EH_2 + NAD^+$$

The recent crystal structure of the native oxidized enzyme, determined at 2.8 Å resolution using cryogenic conditions (*2*), conclusively establishes the identity of this non-flavin redox center as an unusual stabilized sulfenic acid derivative of Cys42 (Cys42-SOH).[1] C42S and C42A mutants lacking this residue (Cys42 is the only cysteine in the protein; refs 3 and 4) have very low activity levels approximately 0.04% that of wild-type enzyme (*5*); flavin reduction by NADH is very rapid, but the $FADH_2$ enzyme is seriously impaired in its ability to catalytically reduce H_2O_2 without the reduced Cys42-thiolate. We have also shown (*6*) that treatment of the native wild-type peroxidase with millimolar concentrations of H_2O_2 leads to inactivation of the cysteinyl redox center and irreversible loss of peroxidase activity; these results were attributed to oxidation of Cys42-SOH to cysteine-sulfinic (Cys42-SO_2H) and/or -sulfonic (Cys42-SO_3H) acid forms. The crystal structures of the Cys42-SO_3H enzyme, both free (*7*) and complexed with NADH (*8*), have been determined at 2.16 and 2.4 Å resolution, respectively.

On the basis of the active-site structure for the NADH peroxidase E(Cys42-SO_3H) complex with NADH, Stehle et

† This work was supported by National Institutes of Health Grant GM-35394 (A.C.), by National Science Foundation Grant INT-9400123 (A.C.), and by the Dutch Foundation for Chemical Research (SON) with financial aid from the Netherlands Organization for Scientific Research (NWO; to J.V.). E.J.C. was the recipient of National Research Service Award GM-16274. This work was also supported by the NIH (RR02231) Stable Isotope Resource Program at Los Alamos. The mass spectrometry facility was supported in part by a center grant, CA-12197, from the National Cancer Institute and by National Science Foundation Grant BIR-94154018.

* To whom correspondence should be addressed at Department of Biochemistry, Wake Forest University Medical Center, Medical Center Boulevard, Winston-Salem, NC 27157. Telephone: (910) 716-3914. Fax: (910) 716-7671. URL: http://invader.bgsm.wfu.edu/.

‡ Wake Forest University Medical Center.

§ Present address: Department of Chemistry, Salisbury State University, 1101 Camden Ave., Salisbury, MD 21801.

‖ Agricultural University, Wageningen.

⊗ Abstract published in *Advance ACS Abstracts,* July 1, 1997.

[1] Abbreviations: Cys42-SOH, Cys42-sulfenic acid; Cys42-SO_2H, Cys42-sulfinic acid; Cys42-SO_3H, Cys42-sulfonic acid; HGAA, peroxidase mutant in which His23, His87, and His258 have been replaced by Gly, Ala, and Ala, respectively; HHAA, peroxidase mutant with Ala replacing His87 and His258; IPTG, isopropyl β-D-thiogalactopyranoside; MOPS, 3-(*N*-morpholino)propanesulfonic acid; TYP, tryptone−yeast extract−phosphate medium; E, oxidized enzyme; EH_2, two-electron reduced enzyme; $E_{inactive}$, peroxide-inactivated peroxidase; Δδ, change in chemical shift; Npx, NADH peroxidase; Nox, NADH oxidase; GR, glutathione reductase; LipDH, lipoamide dehydrogenase.

S0006-2960(97)00799-X CCC: $14.00

al. (*8*) proposed that His10 functions as an acid−base catalyst during H_2O_2 reduction. Mande et al. (*9*), however, have concluded that His10 very likely remains unprotonated throughout the catalytic cycle, since a hydrogen bond exists between the Arg303 guanidinium moiety and the His10 imidazole. Furthermore, we have recently reported (*10*) that His10 is not essential for catalytic activity; rather, this residue functions in part to stabilize the unusual Cys42-SOH redox center within the active-site environment. In an earlier study (*11*) we demonstrated that ^{1}H NMR spectra of the wild-type peroxidase at millimolar concentrations were of surprisingly good quality, given the tetrameric molecular weight of just over 200 000. In order to investigate the Cys42-SOH redox center and its interactions with His10 in the fully active, native enzyme, we have now analyzed the protein labeled independently with [3-^{13}C]Cys and [*ring*-2-^{13}C]His by NMR, and these results form the basis of this report.

EXPERIMENTAL PROCEDURES

Materials and General Methods. L-Cysteine (3-^{13}C, 99 atom %) was purchased from Cambridge Isotope Laboratories, and L-histidine hydrochloride (*ring*-2-^{13}C, approximately 90 atom %) was provided by the Stable Isotopes Resource, Los Alamos National Laboratory. All other chemicals, buffers, and media components were of the best grades available. The procedures used for DNA isolation and manipulation, mutagenesis, and expression of unlabeled NADH peroxidase have been reported previously (*5*,*10*), as have general protocols for enzyme assays and anaerobic spectral titrations (*5*,*12*).

Mutagenesis and Expression. The HGAA triple mutant ($His_{10}Gly_{23}Ala_{87}Ala_{258}$) was constructed in three stages; an H23G, H87A double mutant was generated in the plasmid pNPX14, as recently described for the peroxidase H10Q mutation (*10*), while the H258A mutation was generated in pNPR4, as recently described for the H10A mutant (*10*). The 302 bp *Pst*I−*Xba*I fragment from the p258a plasmid and the 595 bp *Sal*I−*Xba*I fragment from p23,87a were then transferred directly to the pNPX12 expression plasmid (*11*) to give pHGAA. The HHAA double mutant ($His_{10}His_{23}Ala_{87}$-Ala_{258}) was also constructed in pNPX12 from a p87a mutant derivative of pNPX14 and p258a. The R303M mutation was generated in pNPR4, and the 250 bp *Pst*I−*Hin*dIII fragment was ligated into pNPX12 directly. HHAA-R303M was generated by ligating the same *Pst*I−*Hin*dIII fragment from pR303M directly into the pHHAA expression plasmid. In all cases, final expression constructs were checked by both sequence and restriction analysis.

The unlabeled HGAA, HHAA, R303M, and HHAA-R303M mutants were all expressed in *Escherichia coli* JM109(DE3) on induction with IPTG, and the HHAA and HHAA-R303M mutant proteins were purified using the procedure developed for wild-type recombinant NADH peroxidase (*11*).

Preparation of [3-^{13}C]Cys- and [ring-2-^{13}C]His-Labeled Enzymes. The [3-^{13}C]Cys-labeled peroxidase was prepared using the *E. coli* lysogen strain BL21 *cys* (DE3) (*13*), which was kindly provided by Professor August Böck, Universität München. This Cys auxotroph carries a chromosomal copy of the T7 RNA polymerase gene under the control of the *lac*UV5 promoter. The strain was transformed with the pNPX12 expression plasmid encoding the wild-type peroxidase, and an overnight culture was grown at 37 °C with vigorous shaking in a 250-mL flask containing 100 mL of the Cys-labeling medium described in Table 1 plus unlabeled Cys (50 μg/mL), kanamycin (50 μg/mL), and chloramphenicol (50 μg/mL). From this culture 1% inocula were transferred to each of 10 2-L flasks containing 500 mL of the labeling medium plus antibiotics and 9.6 μg/mL [3-^{13}C]-Cys. Once the cultures reached an A_{600} of ∼1.0 under these Cys-limited conditions, they were harvested by centrifugation, and the combined pellets were resuspended in 1 L of fresh labeling medium containing 40 mg of labeled Cys and 0.1 mM IPTG. These two 500-mL cultures were then incubated with shaking for 5 h before harvesting, and the pellets were stored at −80 °C until use. Labeled enzyme was purified as previously described (*11*), except that the resuspended bacteria were homogenized with an SLM/Aminco French press, and the yield of wild-type peroxidase (∼100 mg/5-L culture) was similar to that obtained from cultures grown in TYP medium (*11*).

For the His-labeling studies, the *E. coli* His auxotroph, strain KL719 (provided by Dr. Ian Blomfield, Wake Forest University Medical Center), was converted into a DE3 lysogen [KL719(DE3)] using the kit purchased from Novagen. For preparation of the [^{13}C]His-labeled peroxidase, this strain was transformed with the appropriate pNPX12 derivative (pNPX12, pHHAA, or pHHAA-R303M) and grown overnight in the His-labeling medium (Table 1) containing unlabeled His (100 μg/mL) and chloramphenicol (50 μg/mL). This culture was used to inoculate 5 L of fresh labeling medium containing unlabeled His at only 5 μg/mL; once this culture was grown and harvested as described in the Cys-

Table 1: Composition of Glucose-Rich MOPS Media[a] Used for Preparation of ^{13}C-Labeled NADH Peroxidase

			[3-^{13}C] Cys-labeling (mM)	[*ring*-2-^{13}C] His-labeling (mM)
A.	L-amino acids[b]	Ala	18.7	0.8
		Asp	0.5	0.5
		Cys	0[c]	0.8
		Glu	0.8	0.8
		His	0.6	0[c]
		Ile	12.7	0.4
		Leu	3.1	0.8
		Met	0.7	0.7
		Thr	0.8	0.8
		Val	14.2	0.6
				both media (μM)
B.	nucleosides	adenosine		50
		guanosine		56
		cytidine		48
		uridine		56
		thymidine		55
C.	vitamins	thiamine		10
		pantothenate		20
		riboflavin		5
		pyridoxine		6
		folate		2
		nicotinic acid		20
		biotin		0.8

[a] The glucose−MOPS medium of Neidhardt et al. (*14*) was employed, except that concentrations of $MgCl_2$ and $CaCl_2$ are 0.25 mM and 6.6 μM, respectively. Glucose concentration is 30 mM. [b] Concentrations of L-amino acids and glycine are as given in Wanner et al. (*15*), unless otherwise indicated. [c] Concentrations of Cys and His, respectively, are given in the text.

labeling protocol, the combined pellets were resuspended in 1 L of fresh medium containing 70 mg of [*ring*-2-^{13}C]His. Pellets obtained after 5 h of growth were processed as described for the Cys-labeled protein; pure protein yields for HHAA and HHAA-R303M peroxidases were ~75 mg/5-L culture.

NMR Spectroscopy. Labeled NADH peroxidase samples were prepared for NMR analysis by three cycles of ultrafiltration in 50 mM potassium phosphate buffer at the appropriate pH, without EDTA, using a CM-30 microconcentrator (Amicon). The sample was transferred to a 5-mm NMR tube with 60 μL of D_2O, giving a total sample volume of 0.5−0.75 mL and a protein concentration of 1.5−3 mM (FAD). The final D_2O concentration in the NMR solvent was 8−12%, and the apparent pH values given in the text (7.0 in most cases) are not corrected for the D_2O. For most measurements 0.5 μL of dioxane was added as an internal standard ($\delta = 67.8$ ppm) for ^{13}C spectra. NMR spectra were recorded on a Bruker DPX 400 spectrometer operating at 400.13 and 100.62 MHz for ^{1}H and ^{13}C measurements, respectively, with a sample temperature of 303 ± 0.1 K. ^{13}C measurements were ^{1}H decoupled using a Waltz16 pulse sequence. Spectra were acquired with 60° pulse angles using a 5-mm dual ^{13}C/^{1}H probe and a repetition time of 0.9 s. Acquisition times ranged from 5 to 24 h (20000−100000 transients), and all spectra were recorded under identical settings. In all cases where spectra of the oxidized (E) form of the peroxidase were measured, the enzyme was titrated with substoichiometric H_2O_2 to convert any EH_2 present to E (*11*). The peroxide-inactivated ($E_{inactive}$) and EH_2 forms were generated as previously described (*12*).

Mass Spectrometry. Mass spectrometric analysis was carried out on a Quattro II triple quadrupole mass spectrometer equipped with an electrospray interface. Protein samples (EH_2 and $E_{inactive}$) were dialyzed against H_2O prior to analysis, using CM-30 microconcentrators. Samples were then diluted to a final concentration of 1.2 μM (FAD) in 50% acetonitrile containing 0.1% formic acid and introduced into the electrospray interface at 5 μL/min. Acquisition parameters were adjusted to maximize resolution.

RESULTS

Preparation of [3-^{13}C]Cys-Labeled Peroxidase. Earlier work in this laboratory (*11*) had led to the development of a T7 RNA polymerase-based *E. coli* expression system, and we decided to adapt our wild-type peroxidase expression protocol for this study. Müller et al. (*13*) had developed the *E. coli* BL21 *cys* (DE3) strain, which requires added Cys for growth, in order to allow efficient biosynthetic replacement of the Cys residues in thioredoxin with selenocysteine. In our hands, this Cys auxotroph allowed for efficient growth control mediated by the amounts of exogenous Cys added. We were therefore able to program the culture during the growth phase for a limiting A_{600} of ~1.0 by including labeled Cys at 9.6 μg/mL. The defined medium used in this study is a modified version of the glucose-rich MOPS medium developed by Neidhardt and co-workers (*14,15*), containing all amino acids except Cys plus vitamins and nucleosides. Preliminary NMR analyses indicated that scrambling of the [3-^{13}C]Cys label, especially involving the methyl groups of Ala and the branched-chain amino acids, was suppressed significantly at the relatively high levels of Ala, Val, Ile, and Leu indicated in Table 1. This effect is most likely mediated through end product inhibition of the branched-chain amino acid and Ala biosynthetic pathways from pyruvate (*16*), which can be formed as a consequence of [3-^{13}C]Cys catabolism (*17*) with retention of label. Following this protocol the yield of labeled peroxidase was 100 mg/5-L culture. *E. coli* does not have an NADH peroxidase, so endogenous enzyme expression by the host is not a factor.

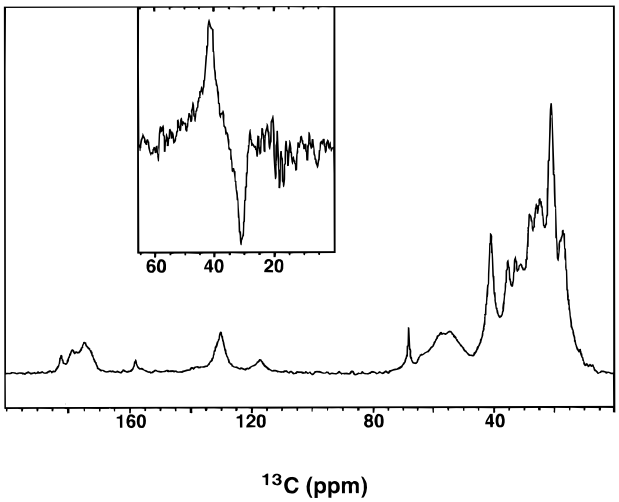

FIGURE 1: ^{13}C NMR spectrum of [3-^{13}C]Cys-labeled NADH peroxidase Cys42-SOH form at pH 7.0, 30 °C. The sample concentration was 3 mM in active sites (FAD), and 55 781 transients were accumulated. Inset: difference spectrum of E minus EH_2 peroxidase forms. The EH_2 sample concentration (FAD) was 3 mM, and 49 943 transients were accumulated.

Peroxidase E and EH_2 Forms. NADH peroxidase contains only one Cys (Cys42) per subunit (*3,4*), and Figure 1 gives the ^{13}C NMR spectrum of the oxidized enzyme (E; Cys42-SOH) labeled with [3-^{13}C]Cys, as obtained with 3 mM enzyme (FAD) at pH 7.0, 30 °C. In experiments similar to that shown in Figure 1, we demonstrated that the wild-type NADH peroxidase sample loses no appreciable activity over 24 h under these conditions. The difference spectrum of labeled minus unlabeled E (data not shown) does indicate that some scrambling of the Cys label has occurred, as evidenced in the 31−38 ppm region attributable to $^{13}C^{\beta}$ contributions from, for example, Ile and Val (*18*). However, a distinct peak also occurs at 41.3 ppm (relative to dioxane at 67.8 ppm), which is essentially absent in difference spectra of the labeled two-electron reduced (EH_2; Cys42-SH) enzyme minus unlabeled E. Although other $^{13}C^{\beta}$ resonances (e.g., Leu) can be observed in the 40−41 ppm range, the $^{13}C^{\beta}$ chemical shift for cystine is 40.2 ppm (*18*), and we tentatively concluded that the chemical shift at 41.3 ppm in E represented the [3-^{13}C]-labeled Cys42-SOH.

Further support for this conclusion is given in Figure 1, in the difference spectrum of labeled E minus labeled EH_2 measured at pH 7.0, 30 °C. The maximum and minimum correspond to chemical shifts of 41.3 and 30.8 ppm, respectively; the 41.3 ppm peak compares very favorably to that observed in the labeled minus unlabeled E difference spectrum and is attributed to Cys42-SOH. The minimum at 30.8 ppm compares favorably with the $^{13}C^{\beta}$ chemical shift of 27 ppm for reduced Cys, reported by Wishart and Sykes (*18*) as an average for Cys residues as identified in 12 known protein structures. Wilson et al. (*19*) have reported pK_a values for Cys32-SH and Cys35-SH in the thioredoxin D26A

Table 2: $^{13}C^{\beta}$ Chemical Shift Values Calculated[a] for Oxidized Forms of Cysteine

compound	$^{13}C^{\beta}$ chemical shift (ppm)
Cys-SH	29.5
Cys-S-OH	39.6
Cys-S(=O)H	48.7
Cys-SS-Cys	38.7
Cys-S(=O)OH	58.8
Cys-S(=O)$_2$OH	56.0

[a] $^{13}C^{\beta}$ chemical shifts were calculated using the C-13 NMR Module for ChemIntosh (SoftShell International; ref 22).

mutant; the protonated thiol $^{13}C^{\beta}$ chemical shifts are ~24.7 ppm, and the thiolate forms are observed at ~28.5 ppm. pK_a values have also been reported for these Cys residues in reduced wild-type thioredoxin (*20*); the protonated thiol $^{13}C^{\beta}$ chemical shifts are 24.3 and 25.9 ppm, respectively, and the corresponding thiolate forms are observed at 27−28 ppm. These comparisons support our assignment of the 30.8 ppm chemical shift given in Figure 1 to the Cys42-SH of the peroxidase EH_2 form; we should emphasize that air oxidation of EH_2 under these conditions is ≤7.5% over a 12-h acquisition period. pH titration of the visible charge-transfer absorbance band of EH_2 indicates that Cys42-SH has an unusually low pK_a of ≤4.5 (*21*); the ^{13}C chemical shift attributed to the EH_2 Cys42-SH does not change on lowering the pH to 5.8 and is consistent with this low pK_a. Measurements at lower pH values were precluded by the formation of an extremely viscous protein gel during concentration.

Calculated Chemical Shift Values for Cys-SH and Derivatives. In order to corroborate these assignments for Cys42-SOH and Cys42-SH of the peroxidase, the $^{13}C^{\beta}$ shifts for Cys and several oxidized derivatives were calculated (Table 2) using the C-13 NMR Module for ChemIntosh (SoftShell International), which is capable of predicting chemical shifts with an overall standard deviation of ±5.5 ppm (*22*). Another limitation is the requirement that all structures be analyzed in their protonated forms. With these provisions in mind, the predicted values for the [3-^{13}C] chemical shifts of Cys-SH and Cys-S-OH are 29.5 and 39.6 ppm, respectively, comparable to the Cys42-SH and Cys42-SOH values of 30.8 and 41.3 ppm in the peroxidase. Furthermore, as pointed out by Kice (*23*) and by Hogg (*24*), sulfenic acids can exist in an S-protonated "sulfoxide" tautomeric form (RS(=O)H), although the O-protonated "sulfenyl" form generally predominates. Tripolt et al. (*25*) applied ^{13}C NMR analysis to determine that the unusually stable 4,6-dimethoxy-1,3,5-triazine-2-sulfenic acid exists only as the sulfenyl tautomer in solution, and Ishii et al. (*26*) recently reached the same conclusion based on spectroscopic analysis of the stable sulfenic acid derivative of thiophenetriptycene-8-thiol. The C-13 NMR Module predicts a chemical shift of 48.7 ppm for the sulfoxide tautomer Cys-S(=O)H, leading us to conclude that the sulfenyl tautomer is preferentially stabilized in the oxidized peroxidase. Finally, although the predicted shift for cystine (38.7 ppm) is similar to that observed for Cys42-SOH (41.3 ppm), the peroxidase contains no disulfides, and the possibility of a redox-active disulfide in the peroxidase has previously been ruled out (*3*,*6*).

Peroxidase $E_{inactive}$ Form. Similar calculations show that oxidation of Cys42-SOH to the Cys42-sulfinic (Cys42-S(=O)OH) and/or Cys42-sulfonic (Cys42-S(=O)$_2$OH) acid states could yield [3-^{13}C] chemical shifts of 58.8 and 56.0 ppm, respectively. We have previously shown that H_2O_2 inactivation of the peroxidase involves irreversible oxidation of Cys42-SOH to the sulfinic and/or sulfonic acid states (*6*), and we therefore undertook the ^{13}C NMR analysis of $E_{inactive}$. As a preliminary, both EH_2 and $E_{inactive}$ were subjected to electrospray mass spectrometric analysis, as shown in Figure 2. The calculated molecular weight for the peroxidase polypeptide, not including the noncovalently bound FAD which dissociates in the acidic solvent (0.1% formic acid in 50% acetonitrile) used for sample introduction into the mass spectrometer, is 49 551 (Cys42 included as Cys-SH; ref 4); the mass determined for reduced peroxidase is 49 559 Da. Similar analysis of the $E_{inactive}$ sample gave a mass of 49 596 Da, representing an increase of 37 Da over the Cys42-SH form. The accuracy of these measurements is to within 0.01% (5 Da); the Cys42-SO_2H and Cys42-SO_3H forms should correspond to 32 Da (m = 49 591 Da) and 48 Da (m = 49 607 Da) increases, respectively, over the E(Cys42-SH) mass of 49 559 Da. While the observed increase of 37 Da is more consistent with Cys42-SO_2H formation, the accuracy of these measurements does not allow us to exclude the possibility of an E(Cys42-SO_3H) structure for $E_{inactive}$.

Figure 3 gives both the full ^{13}C NMR spectrum of Cys-labeled $E_{inactive}$ and the labeled $E_{inactive}$ minus labeled E difference spectrum. The full spectrum confirms the absence of significant line-broadening effects for $E_{inactive}$ relative to E, consistent with the results of spectral (*6*) and structural (*7*,*8*) analyses of $E_{inactive}$ and E(Cys42-SO_3H). The $E_{inactive}$ minus E difference spectrum indicates the loss of the 41.3 ppm resonance attributed previously to Cys42-SOH, while a new maximum appears at 57.0 ppm. On the basis of the mass spectrometric analysis, the C-13 NMR Module prediction, and earlier studies of $E_{inactive}$ (*6*), we assign this new peak to Cys42-SO_2H and/or Cys42-SO_3H. These data not only support our conclusions regarding the usefulness of the C-13 NMR Module predictions but also further substantiate the assignment of the Cys42-SOH structure to the peak at 41.3 ppm. The cumulative shift observed for Cys42-SH to the -SOH and -SO_2H/-SO_3H forms, which corresponds to an overall $\Delta\delta$ of 26.2 ppm, is also consistent with the further deshielding expected to occur on oxidation of the Cys42 sulfur.

An additional observation based on the ^{13}C NMR spectra of the Cys42-SH, Cys42-SOH, and Cys42-SO_2H/-SO_3H forms of the peroxidase concerns the smaller line width for the $E_{inactive}$ derivative (200 Hz) relative to those for Cys42-SH and Cys42-SOH (350 Hz). This indicates that the Cys42 residue in the SO_2H/SO_3H form has increased mobility relative to the thiol and sulfenic acid forms. Cys42-SH and Cys42-SOH have the same line widths, and hence the same mobility.

Construction of HHAA and HHAA-R303M NADH Peroxidase Mutants and [ring-2-^{13}C]His Labeling. The wild-type enzyme contains four His residues including the active-site His10 (*4*,*7*). Inspection of the crystal structure indicates that His23, His87, and His258 are surface-exposed; His23 is the C-terminal residue of helix α1 within the FAD-binding βαβ-fold. We initially constructed and expressed the HGAA triple mutant; although expression was observed at good levels, there was no peroxidase activity in the crude extract. Furthermore, initial purification trials indicated that the expressed protein did not bind FAD tightly, and this mutant was not pursued further. Guided by the primary goal of

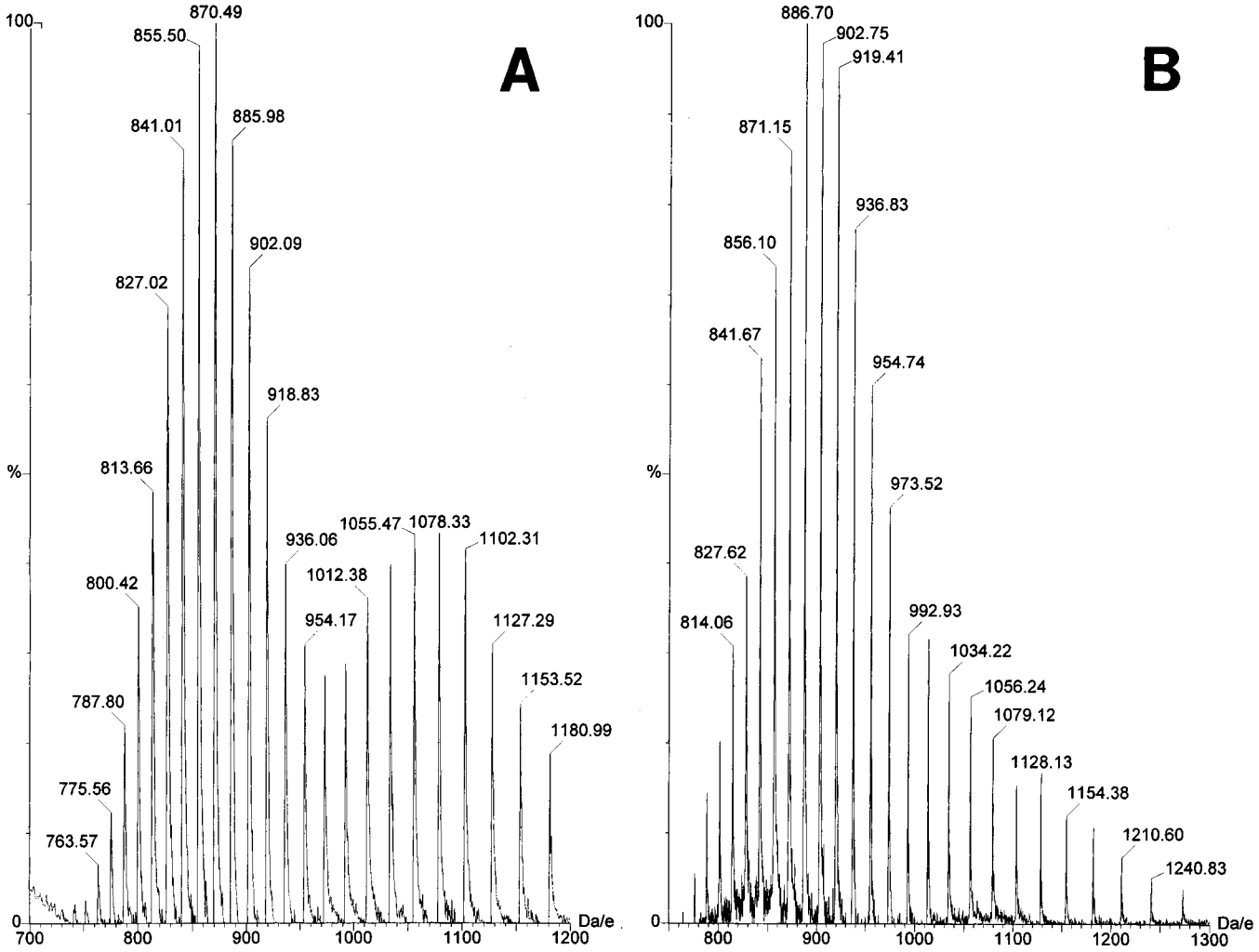

FIGURE 2: Electrospray mass spectra of NADH peroxidase EH_2 (A) and $E_{inactive}$ (B) forms. The charge states for the two forms are indicated. The deconvoluted molecular weights are 49 559 and 49 596, respectively.

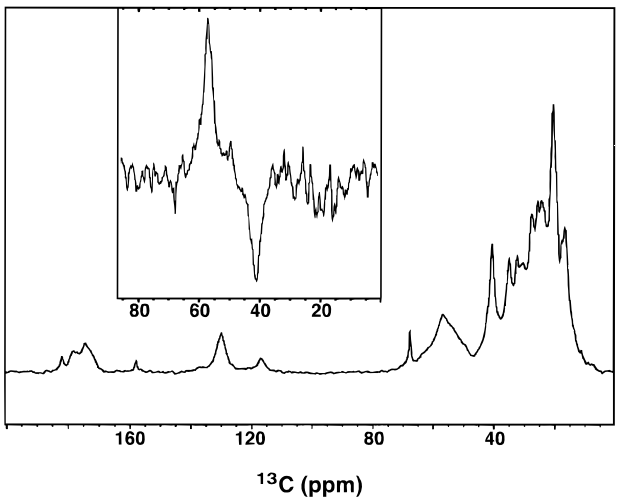

FIGURE 3: ^{13}C NMR spectrum of [3-^{13}C]Cys-labeled NADH peroxidase $E_{inactive}$ form at pH 7.0, 30 °C. The sample concentration (FAD) was 3 mM, and 84 220 transients were accumulated. Inset: difference spectrum of $E_{inactive}$ minus E peroxidase forms. The spectrum of E was taken from Figure 1.

simplifying the ^{13}C His NMR spectral assignments, we constructed and expressed the HHAA mutant. The HHAA peroxidase was purified; the specific activity, UV−visible absorbance and fluorescence spectral properties, and anaerobic titration behavior with NADH were essentially identical to those of the wild-type enzyme (*11*). In order to probe the interaction of His10 with Arg303 (*9*), the R303M derivative of HHAA was constructed and expressed as well. A full characterization of the R303M peroxidase (*27*) is in progress, and these results will be reported in a separate communication.[2] Using the *E. coli* His auxotroph strain KL719(DE3) and the defined medium given in Table 1, we initially prepared the [*ring*-2-^{13}C]His-labeled wild-type and HHAA proteins. The relatively high levels of Ala, Val, Ile, and Leu required to minimize scrambling of the Cys label were not required for His labeling, and the HHAA protein was obtained in a yield of ~75 mg/5-L culture.

HHAA Peroxidase. Figure 4 gives the full ^{13}C NMR spectrum of the HHAA peroxidase in the oxidized (Cys42-SOH) form labeled with [*ring*-2-^{13}C]His, as obtained with 2.3 mM enzyme (FAD) at pH 7.0, 30 °C. Comparison with the unlabeled wild-type enzyme spectrum identifies the new peak at 136.2 ppm, attributed to the C-2 carbons of His10 and His23. Hunkapiller et al. (*28*) demonstrated that the C-2 resonance for the active-site His of α-lytic protease shifts from 134.6 to 137.0 ppm on deprotonation, and Zhang et al. (*29*) reported similar $\Delta\delta$ values (1.9−2.7 ppm) during titration of two of the His residues in glutathione-*S*-transferase isoenzyme 3-3 by ^{13}C NMR. On the basis of the spectrum in Figure 4, it appears that the C-2 resonances

[2] Crane, E. J., III, and Claiborne, A., unpublished observations.

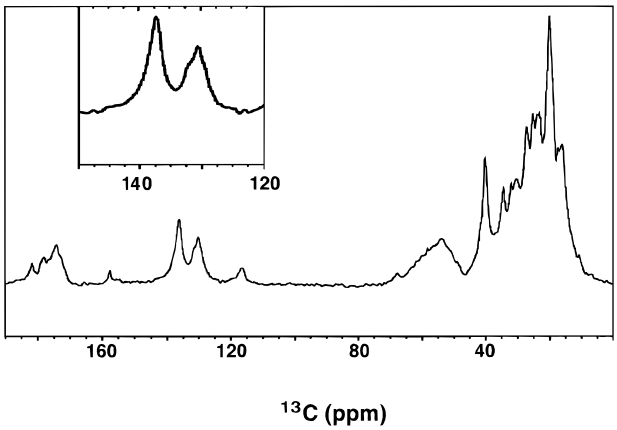

FIGURE 4: ^{13}C NMR spectrum of [*ring*-^{13}C]His-labeled NADH peroxidase HHAA mutant (E form) at pH 7.0, 30 °C. The sample concentration (FAD) was 1.6 mM, and 59 016 transients were accumulated. Inset: the 120−150 ppm region of the spectrum is displayed.

of His10 and His23 in HHAA are not resolved; furthermore the chemical shift of 136.2 ppm suggests that the neutral forms of both His residues predominate at pH 7.0. When the HHAA EH_2 (Cys42-SH) and $E_{inactive}$ (Cys42-SO_2H/-SO_3H) forms are analyzed at pH 7.0 under similar conditions, there is effectively no change in the observed ^{13}C spectrum, indicating that protonation of neither His10 nor His23 is affected by the Cys42 oxidation state. A pH increase with the HHAA E form over the range 5.8−7.8 (data not shown) reveals a narrowing of the peak width from 2.9 to 1.6 ppm, with a small increase in chemical shift from 136.2 to 137.1 ppm; a single, relatively sharp resonance is observed at pH 7.8. The spectrum at pH 5.8 suggests the existence of two nonresolved resonance peaks, one at about 135.3 ppm and one at about 137 ppm. These data suggest that at least one of the His residues in the oxidized enzyme is titrating to some extent in this pH range.

HHAA-R303M Peroxidase. In order to provide an NMR probe of the Arg303-NH2:His10-ND1 interaction indicated by the NADH peroxidase crystal structure (*9*), ^{13}C NMR analysis was also applied to the HHAA-R303M triple mutant labeled with ^{13}C His. Elimination of this hydrogen bond by replacement of Arg303 would be expected to increase the pK_a of His10, leading to a change in the pH-dependent properties of the spectrum. However, the difference spectrum of labeled HHAA minus labeled HHAA-R303M over the range 120−150 ppm at pH 7.0 reveals no significant change, and the pH 6.0 minus pH 8.0 difference spectrum for HHAA-R303M is essentially identical to that observed for HHAA.

DISCUSSION

NADH peroxidase (Npx; $NADH + H^+ + H_2O_2 \rightarrow NAD^+ + 2H_2O$) and the homologous NADH oxidase (Nox; $2NADH + 2H^+ + O_2 \rightarrow 2NAD^+ + 2H_2O$) represent the two peroxide reductases within the flavoprotein disulfide reductase family (*30*,*31*); the major distinguishing feature of Npx and Nox concerns the presence of an unusual active-site Cys-SOH which serves as the non-flavin redox center (*1*,*2*). All other disulfide reductase family members, including glutathione reductase (GR) and lipoamide dehydrogenase (LipDH), contain redox-active cystine disulfides in addition to FAD (*32*); still, comparison of the Npx and GR crystal structures reveals that Cys42-CA of the peroxidase occupies the same position as the charge-transfer Cys63-CA in human erythrocyte GR, when the FAD-binding domains are superimposed (*7*). Of the several partial and complete Npx and Nox sequences available, Cys42 is absolutely conserved; the active-site His10 is also conserved except for the Nox sequence from the archaeon *Methanococcus jannaschii* (*33*), which is a strict anaerobe. While the presence of the active-site His, given the essential role demonstrated for His439′ in *E. coli* GR (*34*) (His444′ in *E. coli* LipDH; ref 32), represents a point of favorable comparison with these disulfide reductases, mechanistic analyses have recently shown (*10*) that His10 is not essential in the peroxidase catalytic cycle. His10 appears to remain unprotonated throughout the reaction (*9*), in direct contrast to the role played by GR His439′ as an acid−base catalyst. In the present study we have applied ^{13}C NMR as a structural probe of the peroxidase active site, focusing on the Cys42-SOH redox center and His10.

Our analysis of Cys42 in the [3-^{13}C]Cys-labeled peroxidase is simplified by the fact that this is the only Cys residue in the protein; the ^{13}C resonance corresponds to the C^{β} atom bonded directly to the Cys42-SOH sulfur. Furthermore, we have previously shown (*3*) that two-electron reduction of E → EH_2 corresponds to the reduction of Cys42-SOH → Cys42-SH. Wishart and Sykes (*18*) have compiled a ^{13}C chemical shift index useful for the identification and location of protein secondary structural elements; the backbone "coil" $^{13}C^{\beta}$ range for Cys (oxidized; 40.2 ± 0.7 ppm, relative to dioxane) is 13.2 ppm downfield from that for Cys (reduced; 27.0 ± 0.7 ppm), suggesting that ^{13}C difference measurements with the peroxidase E and EH_2 forms should be informative. Two other major experimental factors include the quality of the ^{13}C-labeled peroxidase spectrum, which is excellent considering the tetrameric molecular weight of just over 200 000, and the stability of EH_2 under aerobic conditions during acquisition periods of up to 12 h. Experimentally the peroxidase E minus EH_2 difference spectrum gives chemical shift values of 41.3 and 30.8 ppm for Cys42-SOH and Cys42-SH, respectively; the observed $\Delta\delta$ of 10.5 ppm on oxidation−reduction is comparable to that expected on the basis of the chemical shift index values compiled by Wishart and Sykes (*18*). Thus it appears that oxidation of Cys42-SH → Cys42-SOH is accompanied by a $\Delta\delta$ very similar to that for Cys-SS-Cys formation.

Chandrasekhar et al. (*35*) have reported the complete aliphatic ^{13}C NMR assignments for thioredoxin in its Cys (reduced) and Cys-SS-Cys forms at pH 5.7. The Cys32 and Cys35 $^{13}C^{\beta}$ chemical shifts of 24.3 and 25.9 ppm in the reduced protein are consistent with protonated Cys-SH; the respective pK_a values for the wild-type protein were reported by Jeng et al. (*20*) to be 7.5 and 9.5. In the oxidized protein, the Cys32 $^{13}C^{\beta}$ value shifts downfield to 41.9 ppm ($\Delta\delta$ = 17.6 ppm); in contrast the Cys35 $^{13}C^{\beta}$ is assigned a chemical shift of 32.5 ppm in oxidized thioredoxin. The 1.68 Å crystal structure of thioredoxin (*36*) shows that the Cys32−Cys35 disulfide is located at the N-terminus of an α-helix, and Chandrasekhar et al. (*35*) have attributed the significantly different $^{13}C^{\beta}$ shifts for the two Cys residues to a greater helical character at Cys35 in the oxidized protein. Wilson et al. (*19*) determined $^{13}C^{\beta}$ chemical shifts of 25−26 ppm for both Cys residues in the reduced D26A thioredoxin mutant at pH 7.0, consistent with Cys-SH protonation; both

were reported to titrate with pK_a values of 7.8−7.9 to new positions at 27−29 ppm. The measurements of Jeng and Dyson (*37*) with the reduced D26A thioredoxin also indicate that the pK_a values for Cys32-SH and Cys35-SH are between 7.5 and 8.0.

The chemical shift of 30.8 ppm determined for the reduced Cys42 peroxidase is fully consistent with stabilization of the Cys42-thiolate, and the absence of any change in the $^{13}C^{\beta}$ shift over the pH range 5.8−7.0 supports the earlier conclusion (*21*) that the Cys42-SH pK_a is ≤4.5. As described above for the active-site Cys35 in oxidized thioredoxin, NMR shifts are dependent on both secondary structure and local environment. Cys42 of the peroxidase is located immediately ahead of the short α2 helix (Gly43−Glu49), but careful examination of the structure suggests that the α2 helix dipole has little impact on the electrostatic environment of Cys42. The 2.8 Å structure of the native enzyme identifies two types of interactions between Cys42-SOH and other active-site elements (*1*,*2*). These include hydrogen bonds between the sulfenic acid oxygen atom and His10-NE2 (3.5 Å) and possibly with the ribityl-O2′F of the FAD (3.5 Å). The second interaction involves a charge transfer between the Cys42-SOH oxygen and the electron-deficient isoalloxazine ring of FAD. The oxygen atom approaches to within 3.5 Å of FAD-C4aF, 3.2 Å of FAD-N1F, and 3.2 Å of FAD-C10aF; the corresponding distances for the Cys42 sulfur are 3.7, 4.1, and 3.6 Å. On the basis of the strong charge-transfer absorbance of the Cys42-SOH form of the H10Q peroxidase mutant, we have suggested (*10*) that Cys42-SOH may be stabilized in its anionic sulfenate form, maximizing its potential as a charge-transfer donor to FAD. Our ^{13}C NMR data with the Cys42-labeled peroxidase do not, however, provide further information on this point.

Tripolt et al. (*25*) have reported the spectroscopic properties and X-ray crystal structure for the stable 4,6-dimethoxy-1,3,5-triazine-2-sulfenic acid; more recently Ishii et al. (*26*) have provided the characterization and crystal structure for thiophenetriptycene-8-sulfenic acid. To our knowledge these data include the only ^{13}C NMR analyses of any sulfenic acids. The chemical shift for the C-2 carbon (bonded to -SOH) in the triazine-2-SOH is 190.3 ppm, while the equivalent ring C-4 and C-6 carbons (bonded to OCH_3) appear at 170.9 ppm. The C-13 NMR Module used to predict chemical shifts in the present study (see Results) calculates values of 196.2 and 177.9 ppm for the C-2 and C-4, C-6 positions, respectively, providing an additional measure of confidence (standard deviation = ±5.5 ppm) in the additivity-based algorithm (*22*). Using this program we have estimated $^{13}C^{\beta}$ chemical shifts for free Cys-SH and cystine, as well as the sulfenyl and sulfoxide tautomers of Cys-SOH, and for Cys-SO_2H and Cys-SO_3H. Our NMR data support the sulfenic acid structure for the monooxidized form of Cys42 (41.3 versus 39.6 ppm, predicted) as well as the sulfinic/sulfonic acid structure for the Cys42 derivative in $E_{inactive}$ (57.0 versus 56.0−58.8 ppm, predicted).

We have demonstrated that, as expected based on the peroxidase crystal structure (*7*), the surface-exposed His87 and His258 are not essential for activity. More surprising is the observation that the HGAA mutant does not bind FAD; although the cause of this coenzyme binding and/or protein stability problem is not known, it should be emphasized that His23 is the C-terminal residue of the α1 helix within the FAD-binding $\beta\alpha\beta$-fold. In triosephosphate isomerase (*38*) and barnase (*39*), for example, protonated His residues at the C-termini of the respective helices afford significant stabilization of these secondary structural elements by electrostatic interaction with the helix dipole. Working with the peroxidase HHAA mutant, our ^{13}C NMR analysis of the His-labeled protein does not provide for the resolution of the His10 and His23 resonances, although there is evidence for titration of one or both components over the pH range 5.8−7.8, leading to a single sharp peak at 136.7 ppm. We tentatively conclude that these changes are attributable to deprotonation of His23, which is surface-exposed, does not appear to interact directly with any other protein residues (His23-NE2 is 3.9 Å from Glu314-OE2), and is, as stated above, located at the helix α1 C-terminus.

His10, in contrast, is inaccessible to solvent in both the E(Cys42-SO_3H) and C42S mutant structures (*9*), interacts directly with both Arg303 and the Cys42-SOH oxygen in the native E(Cys42-SOH) structure (*2*), and is the second residue in the α1 helix. Both the hydrogen-bond interaction with Arg303 and the location within the N-terminal helix region (*40*) should contribute to stabilization of the neutral His10 imidazole, thus supporting our conclusion that the pH-dependence of the His resonance in the HHAA peroxidase mutant is likely due to deprotonation of His23. And, while we observe that replacement of Arg303 has no significant effect on the ^{13}C His NMR spectrum of the HHAA mutant, we have also shown that the Cys42-SH pK_a in the EH_2 form of the R303M mutant is increased from a value of ≤4.5 in wild-type enzyme to 8.5.[2] Additional structural studies are currently being carried out with Dr. Wim Hol, University of Washington, in order to address the questions raised by these observations.

These active-site considerations serve to further distinguish the two peroxide reductases from GR, LipDH, and other flavoprotein disulfide reductases. In the crystal structures of GR (*41*) and LipDH (*42*), it has been pointed out that the redox-active disulfides exist in strained conformations which may facilitate reduction to the EH_2 state. This is clearly not the case in Npx or Nox, since the non-flavin redox center is Cys-SOH, not a disulfide. The active-site His467′ of human erythrocyte GR is located in a bend which leads into the C-terminal 3_{10}-helix of the polypeptide; the imidazole nitrogens are hydrogen bonded to the Glu472′ side chain and Sol70, respectively (*41*). Spectral pH titrations of the charge-transfer absorbance of the yeast GR EH_2 form give a pK_a for the conserved active-site His456′ (*43*) of 9.2 (*44*); Hopkins and Williams (*45*) obtained a value of 9.5 for His444′ in a similar titration of the *E. coli* LipDH C44S mutant. Again there is a direct contrast with the location of His10 within the Npx and Nox polypeptides, its electrostatic and hydrogen-bonding environment, and its role in catalysis (*1*,*10*).

The combination of this NMR characterization of the Cys-SOH redox center of the NADH peroxidase and the high-resolution crystallographic analysis of the native oxidized enzyme should provide further insights into the molecular basis of protein−sulfenic acid stabilization and function not only in Npx and Nox, but also in redox-regulated DNA-binding proteins such as OxyR (*46*) and nuclear factor I (*47*), for which Cys-SOH centers have also been proposed.

ACKNOWLEDGMENT

We thank Dr. August Böck, Universität München, for providing the *E. coli* BL21 *cys* (DE3) strain, Dr. Derek Parsonage, Dr. Paul Ross, and Dr. Ian Blomfield, Wake Forest University Medical Center, for preparing the KL719 *his* (DE3) strain and for helpful discussions on media selection and mutagenesis, and Dr. Willem van Berkel, Agricultural University, Wageningen, for providing access to his laboratory facilities and his help during the NMR work. We thank Dr. Mike Thomas and Mr. Mike Samuel, Wake Forest University Medical Center, for providing the mass spectrometry analyses and for helpful discussions.

REFERENCES

1. Claiborne, A., Crane, E. J., III, Parsonage, D., Yeh, J. I., Hol, W. G. J., and Vervoort, J. (1997) in *Flavins and Flavoproteins 1996* (Stevenson, K. J., Massey, V., and Williams, C. H., Jr., Eds.), in press.
2. Yeh, J. I., Claiborne, A., and Hol, W. G. J. (1996) *Biochemistry 35*, 9951−9957.
3. Poole, L. B., and Claiborne, A. (1988) *Biochem. Biophys. Res. Commun. 153*, 261−266.
4. Ross, R. P., and Claiborne, A. (1991) *J. Mol. Biol. 221*, 857−871.
5. Parsonage, D., and Claiborne, A. (1995) *Biochemistry 34*, 435−441.
6. Poole, L. B., and Claiborne, A. (1989) *J. Biol. Chem. 264*, 12330−12338.
7. Stehle, T., Ahmed, S. A., Claiborne, A., and Schulz, G. E. (1991) *J. Mol. Biol. 221*, 1325−1344.
8. Stehle, T., Claiborne, A., and Schulz, G. E. (1993) *Eur. J. Biochem. 211*, 221−226.
9. Mande, S. S., Parsonage, D., Claiborne, A., and Hol, W. G. J. (1995) *Biochemistry 34*, 6985−6992.
10. Crane, E. J., III, Parsonage, D., and Claiborne, A. (1996) *Biochemistry 35*, 2380−2387.
11. Parsonage, D., Miller, H., Ross, R. P., and Claiborne, A. (1993) *J. Biol. Chem. 268*, 3161−3167.
12. Crane, E. J., III, Parsonage, D., Poole, L. B., and Claiborne, A. (1995) *Biochemistry 34*, 14114−14124.
13. Müller, S., Senn, H., Gsell, B., Vetter, W., Baron, C., and Böck, A. (1994) *Biochemistry 33*, 3404−3412.
14. Neidhardt, F. C., Bloch, P. L., and Smith, D. F. (1974) *J. Bacteriol. 119*, 736−747.
15. Wanner, B. L., Kodaira, R., and Neidhardt, F. C. (1977) *J. Bacteriol. 130*, 212−222.
16. Umbarger, H. E. (1996) in *Escherichia coli and Salmonella: Cellular and Molecular Biology* (Neidhardt, F. C., Curtiss, R., III, Ingraham, J. L., Lin, E. C. C., Low, K. B., Magasanik, B., Reznikoff, W. S., Riley, M., Schaechter, M., and Umbarger, H. E., Eds.) 2nd ed., Vol. 1, pp 442−457, American Society for Microbiology, Washington, DC.
17. Voet, D., and Voet, J. G. (1990) *Biochemistry*, p 687, John Wiley & Sons, New York.
18. Wishart, D. S., and Sykes, B. D. (1994) *J. Biomol. NMR 4*, 171−180.
19. Wilson, N. A., Barbar, E., Fuchs, J. A., and Woodward, C. (1995) *Biochemistry 34*, 8931−8939.
20. Jeng, M.-F., Holmgren, A., and Dyson, H. J. (1995) *Biochemistry 34*, 10101−10105.
21. Poole, L. B., and Claiborne, A. (1986) *J. Biol. Chem. 261*, 14525−14533.
22. Fürst, A., and Pretsch, E. (1990) *Anal. Chim. Acta 229*, 17−25.
23. Kice, J. L. (1980) *Adv. Phys. Org. Chem. 17*, 65−181.
24. Hogg, D. R. (1990) in *The Chemistry of Sulphenic Acids and Their Derivatives* (Patai, S., Ed.) pp 361−402, John Wiley & Sons, New York.
25. Tripolt, R., Belaj, F., and Nachbaur, E. (1993) *Z. Naturforsch. 48B*, 1212−1222.
26. Ishii, A., Komiya, K., and Nakayama, J. (1996) *J. Am. Chem. Soc. 118*, 12836−12837.
27. Crane, E. J., III, and Claiborne, A. (1997) in *Flavins and Flavoproteins 1996* (Stevenson, K. J., Massey, V., and Williams, C. H., Jr., Eds.), in press.
28. Hunkapiller, M. W., Smallcombe, S. H., Whitaker, D. R., and Richards, J. H. (1973) *Biochemistry 12*, 4732−4743.
29. Zhang, P., Graminski, G. F., and Armstrong, R. N. (1991) *J. Biol. Chem. 266*, 19475−19479.
30. Claiborne, A., Miller, H., Parsonage, D., and Ross, R. P. (1993) *FASEB J. 7*, 1483−1490.
31. Claiborne, A., Ross, R. P., Ward, D., Parsonage, D., and Crane, E. J., III (1994) in *Flavins and Flavoproteins 1993* (Yagi, K., Ed.) pp 587−596, de Gruyter, New York.
32. Williams, C. H., Jr. (1992) in *Chemistry and Biochemistry of Flavoenzymes* (Müller, F., Ed.) Vol. III, pp 121−211, CRC Press, Boca Raton, FL.
33. Bult, C. J., White, O., Olsen, G. J., Zhou, L., Fleischmann, R. D., Sutton, G. G., Blake, J. A., FitzGerald, L. M., Clayton, R. A., Gocayne, J. D., Kerlavage, A. R., Dougherty, B. A., Tomb, J.-F., Adams, M. D., Reich, C. I., Overbeek, R., Kirkness, E. F., Weinstock, K. G., Merrick, J. M., Glodek, A., Scott, J. L., Geoghagen, N. S. M., Weidman, J. F., Fuhrmann, J. L., Nguyen, D., Utterback, T. R., Kelley, J. M., Peterson, J. D., Sadow, P. W., Hanna, M. C., Cotton, M. D., Roberts, K. M., Hurst, M. A., Kaine, B. P., Borodovsky, M., Klenk, H.-P., Fraser, C. M., Smith, H. O., Woese, C. R., and Venter, J. C. (1996) *Science 273*, 1058−1073.
34. Reitveld, P., Arscott, L. D., Berry, A., Scrutton, N. S., Deonarain, M. P., Perham, R. N., and Williams, C. H., Jr. (1994) *Biochemistry 33*, 13888−13895.
35. Chandrasekhar, K., Campbell, A. P., Jeng, M.-F., Holmgren, A., and Dyson, H. J. (1994) *J. Biomol. NMR 4*, 411−432.
36. Katti, S. K., LeMaster, D. M., and Eklund, H. (1990) *J. Mol. Biol. 212*, 167−184.
37. Jeng, M.-F., and Dyson, H. J. (1996) *Biochemistry 35*, 1−6.
38. Lodi, P. J., and Knowles, J. R. (1993) *Biochemistry 32*, 4338−4343.
39. Šali, D., Bycroft, M., and Fersht, A. R. (1988) *Nature 335*, 740−743.
40. Hol, W. G. J. (1985) *Prog. Biophys. Mol. Biol. 45*, 149−195.
41. Karplus, P. A., and Schulz, G. E. (1987) *J. Mol. Biol. 195*, 701−729.
42. Mattevi, A., Schierbeek, A. J., and Hol, W. G. J. (1991) *J. Mol. Biol. 220*, 975−994.
43. Collinson, L. P., and Dawes, I. W. (1995) *Gene 156*, 123−127.
44. Sahlman, L., and Williams, C. H., Jr. (1989) *J. Biol. Chem. 264*, 8033−8038.
45. Hopkins, N., and Williams, C. H., Jr. (1995) *Biochemistry 34*, 11757−11765.
46. Kullik, I., Toledano, M. B., Tartaglia, L. A., and Storz, G. (1995) *J. Bacteriol. 177*, 1275−1284.
47. Bandyopadhyay, S., and Gronostajski, R. M. (1994) *J. Biol. Chem. 269*, 29949−29955.

BI9707990